ACS SENSORS

Letter

pubs.acs.org/acssensors

Marangoni Convection Assisted Single Molecule Detection with Nanojet Surface Enhanced Raman Spectroscopy

Te-Wei Chang,[†] Xinhao Wang,[‡] Amirreza Mahigir,[∥] Georgios Veronis,[∥] Gang Logan Liu,[*,‡] and Manas Ranjan Gartia[*,§]

[†]Intel Corporation, Ronler Acres Campus, 2501 NW 229th Ave, Hillsboro, Oregon 97124, United States

[‡]Department of Electrical and Computer Engineering, University of Illinois at Urbana−Champaign, Urbana, Illinois 61801 United States

[§]Department of Mechanical and Industrial Engineering, Louisiana State University, Baton Rouge, Louisiana 70803, United States

[∥]School of Electrical Engineering and Computer Science, Louisiana State University, Baton Rouge, Louisiana 70803, United States

Supporting Information

ABSTRACT: Many single-molecule (SM) label-free techniques such as scanning probe microscopies (SPM) and magnetic force spectroscopies (MFS) provide high resolution surface topography information, but lack chemical information. Typical surface enhanced Raman spectroscopy (SERS) systems provide chemical information on the analytes, but lack spatial resolution. In addition, a challenge in SERS sensors is to bring analytes into the so-called "hot spots" (locations where the enhancement of electromagnetic field amplitude is larger than 10^3). Previously described methods of fluid transport around hot spots like thermophoresis, thermodiffusion/Soret effect, and electrothermoplasmonic flow are either too weak or detrimental in bringing new molecules to hot spots. Herein, we combined the resonant plasmonic enhancement and photonic nanojet enhancemnet of local electric field on nonplanar SERS structures, to construct a stable, high-resolution, and below diffraction limit platform for single molecule label-free detection. In addition, we utilize Marangoni convection (mass transfer due to surface tension gradient) to bring new analytes into the hotspot. An enhancement factor of $\sim 3.6 \times 10^{10}$ was obtained in the proposed system. Rhodamine-6G (R6G) detection of up to a concentration of 10^{-12} M, an improvement of two orders of magnitude, was achieved using the nanojet effect. The proposed system could provide a simple, high throughput SERS system for single molecule analysis at high spatial resolution.

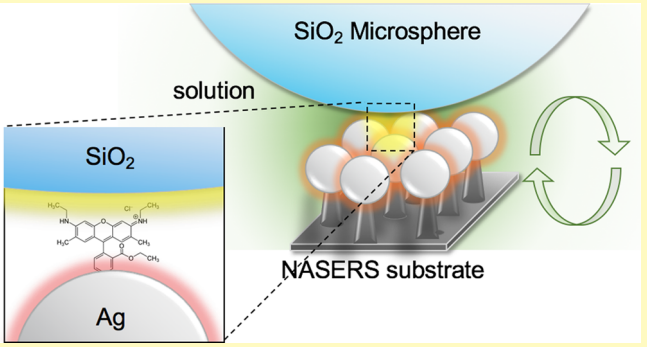

KEYWORDS: *Raman spectroscopy, Marangoni convection, single molecule, nanojet, SERS, enhancement factor, hot spot*

Many single-molecule (SM) techniques such as single-molecule fluorescence spectroscopies,[1−5] scanning probe microscopies (SPM),[6−8] magnetic force spectroscopies,[9,10] and optical tweezers[11] can provide information about the surface topography, molecular electronic density distribution and electronic states, or single molecule under stretching or torsional loading. However, most of these techniques seldom provide chemical information on the analyte under study. Single-molecule Raman spectroscopy can provide a chemical fingerprint of a molecular system since it represents molecular vibrations.[12,13] However, typical Raman microscopy/spectroscopy systems are diffraction limited and lack spatial resolution to observe single molecules.[14] To observe a single molecule at high spatial resolution, recently Raman spectroscopy has been recently combined with atomic force microscopy (AFM) probe to perform tip-enhanced Raman spectroscopy (TERS).[15,16] However, due to the scanning approach employed in TERS, the throughput of the system is low.

Another challenge associated with Raman spectroscopy is its lower scattering cross sections (10^{-25} to 10^{-30} cm^{-1} compared to 10^{-16} cm^{-1} for the fluorescence emission), which hinders the successful application of this technique to detect molecules at low concentration. Surface enhanced Raman spectroscopy (SERS) circumvents this problem by increasing the effective scattering cross-section of the molecules near a metallic nanostructure with the generation of high electromagnetic field.[17,18] In addition to the electromagnetic enhancement (EM), the interaction between metal-molecule electron densities (charge-transfer mechanism (CM)) also contributes to the enhancement of effective Raman scattering cross-section.[19] The typical enhancement of the Raman signal can be calculated to be $|E(\lambda_{ex})|^2|E(\lambda_{RamanScattering})|^2 \sim |E|^4$ where $E(\lambda_{ex})$ is the enhanced electric field at the excitation

Received: June 25, 2017
Accepted: July 14, 2017
Published: July 14, 2017

DOI: 10.1021/acssensors.7b00427
ACS Sens. XXXX, XXX, XXX−XXX

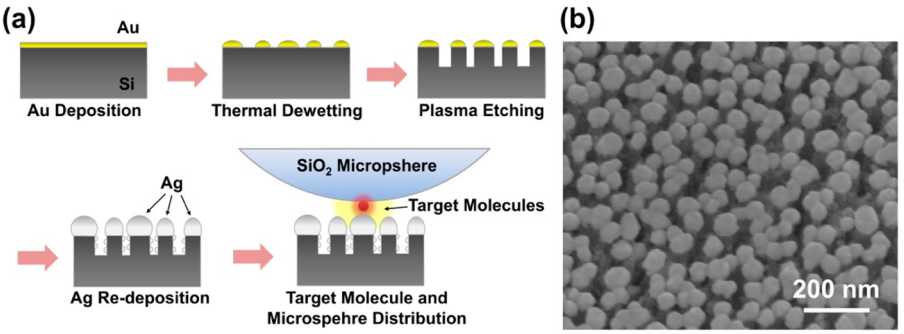

Figure 1. Fabrication of NASERS device. (a) Schematic of the microfabrication steps to prepare the NASERS device. (b) SEM image showing the nanomushroom Ag capped nanopillar structure of the SERS sensor.

wavelength, and $E(\lambda_{\text{RamanScattering}})$ is the enhanced electric field at the emitted Raman scattering wavelength of the molecule (which can be approximated to be the fourth power of incident electric field at the location of the probe molecule).[20]

Initial SERS experiments were peformed with colloidal metallic nanoparticles which provided the "hotspots" (local areas with optical electromagnetic field enhancement factor between 10^5 and 10^{10}) mainly due to the random aggregation of nanoparticles.[21] However, due to the randomness of the aggregation behavior, the results were challenging to replicate, and there is large variation in the SERS intensity within the same batches.[21] With the advancement of microfabrication approaches such as e-beam lithography, focused ion beam milling, and nanosphere lithography, SERS substrates with regular nanostructures were fabricated to improve the repeatability of the results.[22−24] However, simple, low-cost, and reliable fabrication methods to fabricate SERS substrates to perform single molecule detection at high throughput are still challenging to accomplish.

A new approach called "photonic nanojet" was shown computationally to achieve subwavelength confinement of light using dielectric microspheres and microscale cylinders.[25] The results showed that the NASERS system is capable of achieving 3−4 orders of magnitude higher intensity of the local electric field in addition to attaining a smaller incident laser spot size.[25] Subsequently, it was proposed that a three-dimensional subwavelength confinement of optical fields can also be achieved in photonic nanojet systems by an incident Gaussian beam instead of plane wave incident light.[26] Combining these two properties, SERS enhancement factor of $\sim 10^2$ has been achieved on planar Si geometries.[27]

Molecular positioning in a hot spot is important in single-molecule surface enhanced Raman spectroscopy (SMSERS), since enhancement factors are non uniform within individual hot spots and across a SERS substrate.[28] Resonant molecules require enhancement factors of at least $\sim 10^7 - 10^8$ and nonresonant molecules require enhancement factors of at least $\sim 10^9 - 10^{11}$ for single molecule observation in Raman spectroscopy experiments.[14,29,30] Apart from the enhancement factor, it is important to transport the molecules in to the hot spots. Some of the available methods to bring analytes into the hot spots can be broadly categorized into two types: (1) passive methods (e.g., hydrophobic surface,[31] diffusion) and (2) active methods (electrokinetic,[32] optical trap,[33−35] microfluidics,[32] nanofluidics,[36] thermophoresis/thermodiffusion/Soret effect,[37−39] electrothermoplasmonic flow[40]). Previously superhydrophobic artificial surfaces have been combined with nanoplasmonic structures to preconcentrate and localize few molecules (attomolar or 10^{-18} mol/L concentration) to detect using SERS.[31] At the plasmonic hot spot, due to the high electromagnetic field, the molecules will experience two kinds of forces: the gradient force (attractive), which acts in the direction of low electromagnetic field to high electromagnetic field, will try to pull the molecule toward the hot spot.[34] On the other hand, the scattering force (repulsive) will push the molecule out of the hot spot.[34] Due to high EM field, the plasmonic hot spot will be at a higher temperature than the surroundings. Since molecules move from higher temperature to lower temperature (positive Soret effect or moving along the temperature gradient), the molecules will experience another force due to the Soret effect, and will be pushed away from the hot plasmonic surface. Furthermore, such thermoplasmonic convection is relatively weak (∼10−1000 nm/s), and the Brownian motions ($\sim k_B T$) are confined to a few square nanometers area. Since it is pushing away the molecules out of the high temperature regions, it will not assist in bringing new molecules to the hot spot areas. In microfluidics, nanofluidics, and other diffusion processes, the flow terms can be separated into the convection term and the diffusion term. Convection varies as $\sim u\frac{\partial u}{\partial x} \approx \frac{U_\infty^2}{L}$, and the diffusion term varies as $\sim \nu\frac{\partial^2 u}{\partial x^2} \approx \frac{U_\infty}{L^2}$, where ν is the kinematic viscosity (for water at 20 °C it is 10^{-6} m^2 s^{-1}), U_∞ is the fluid velocity, and L is the characteristic length. For a characteristic length of 100 nm and flow velocity between 1 nm/s and 100 μm/s, the diffusion term will always dominate the convection term (Figure S-1). For such characteristic length, the convection and diffusion term will be comparable only when the flow velocity is extremely large (∼10 m/s). Electrothermoplasmonic (ETP)[40] flow using thermophoresis and AC electric field can produce a velocity of ∼100 μm/s; however, the flow will still be diffusion limited.

Here we combined the resonant plasmonic enhancement approach and nonresonant photonic nanojet enhancement approach on nonplanar SERS structures, to fabricate a high-resolution and below diffraction limit platform for single molecule label-free detection. In addition, we utilized Marangoni convection (mass transfer due to surface tension gradient) to bring new analytes into the hotspot. In our previous study, we reported the fabrication of wafer-scale SERS substrates with enhancement factors of 10^8 based on the thermal dewetting technique.[41] With placing dielectric microspheres on such devices, it is expected to increase the enhancement factor as well as confine the incident field. Furthermore, the effect of thermal gradient was analyzed and the Marangoni effect was verified to be another factor

DOI: 10.1021/acssensors.7b00427
ACS Sens. XXXX, XXX, XXX−XXX

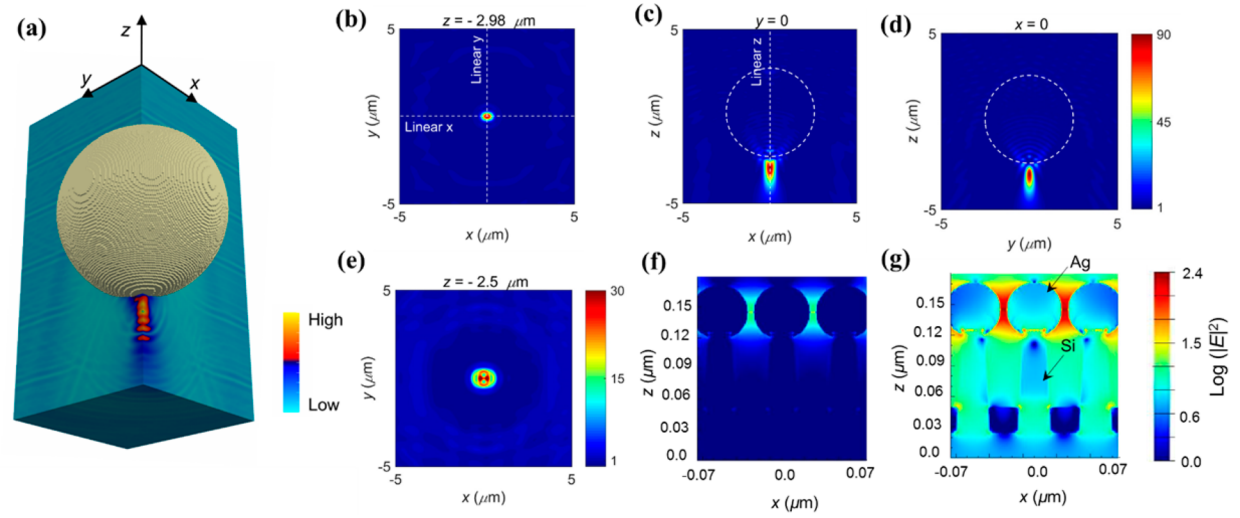

Figure 2. FDTD simulation showing the enhanced electromagnetic field due to the nanojet effect. (a) 3D electromagnetic field distribution at the bottom of a 5 μm SiO_2 microsphere from the excitation of a Gaussian beam at the top of the microsphere. (b) Electric field in the *xy*-plane at a position 480 nm below the bottom of the sphere. (c) Electric field in the *xz*-plane; the microsphere is shown by dotted line; the line along which the linear electric field profile along the *z*-direction is extracted is also shown by a dotted line. (d) Electric field in the *yz*-plane. (e) Electric field in the *xy*-plane at the bottom of the sphere. (f) Electromagnetic field distribution (logarithmic scale) on the SERS substrate in the absence of microsphere (no nanojet effect). (g) Electromagnetic field distribution (logarithmic scale) on the SERS substrate in the presence of microsphere (with nanojet effect).

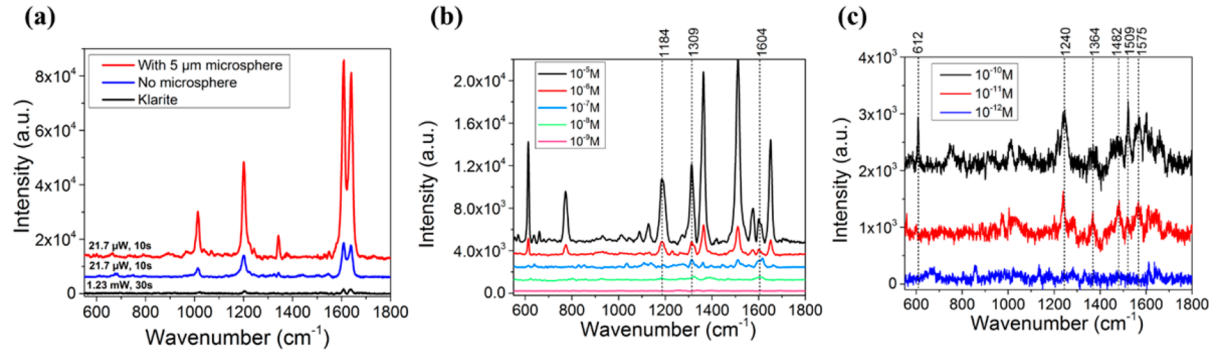

Figure 3. Effect of nanojet on Raman spectra using the NASERS system. (a) Raman spectra of BPE molecule with (red curve) and without (blue curve) nanojet effect; for comparison, SERS spectrum obtained from commercial Klarite substrate is also presented (black curve). For the SERS spectrum with and without microsphere, laser power of 21.7 μW and integration time of 10 s were used, and for the SERS spectrum on Klarite substrate laser power of 1.23 mW and integration time of 30 s were used. (b) SERS spectra of R6G molecule at concentrations of 10^{-5}–10^{-9} M in the absence of nanojet effect. The limit of detection was 10^{-8} M. (c) SERS spectra of R6G molecule at concentrations of 10^{-12}–10^{-10} M in the presence of nanojet effect. The limit of detection was 10^{-12} M.

contributing to the enhancement. In addition to providing enhancement in the Raman signal, the platform will reduce the detection volume by confining the incident wave within a femtoliter (~0.2 fL) (Figure S-2) due to the nanojet effect.

Figure 1a shows schematically the fabrication steps of the nanojet assisted SERS (NASERS) device. First, a 6 nm gold thin-film was deposited on cleaned silicon wafer. Subsequently, the rapid thermal annealing method was applied to perform thermal dewetting of the thin film in order to achieve islands of Au nanoparticles (AuNPs). In order to control the gap size among the particles, and improve the hot spot density, a thick layer (50 nm) of silver was deposited. The scanning electron microscopy (SEM) image of the fabricated SERS substrate is shown in Figure 1b. The SEM shows a mushroom-like structure with Ag cap on top of the Au nanoparticles. The small distance between the nanoparticles is ideal for creating high electromagnetic field (hot spot) leading to better SERS performance.

The finite difference time domain (FDTD) simulation results of the nanojet effect on the proposed system is shown in Figure 2. The excitation beam was modeled as a Guassian beam. To create the nanojet effect, a SiO_2 microsphere with diameter of 5 μm was drop casted on the SERS substrate. The beam width of 6.06 μm (corresponding to 20x objective) was measured from the experimental setup and used in the FDTD simulations. The center of the microsphere was modeled to be the focal plane of the simulation setup. The simulation results (Figures 2a–e and S-2) show that the beam width of the incident beam is reduced to 0.506 × 0.371 × 1.165 μm^3 in *x*, *y*, and *z* leading to femtoliter excitation volume. Due to this three-dimensional confinement, it is expected that the electromagnetic field generated on the SERS substrate will be altered. In fact, Figure 2f and g shows a comparison between the electromagnetic field (in logarithmic scale) generated on the SERS substrate with and without microspheres. The results showed a two-orders of magnitude enhancement in the intensity of the electromagnetic field strength due the presence of microspheres.

DOI: 10.1021/acssensors.7b00427
ACS Sens. XXXX, XXX, XXX–XXX

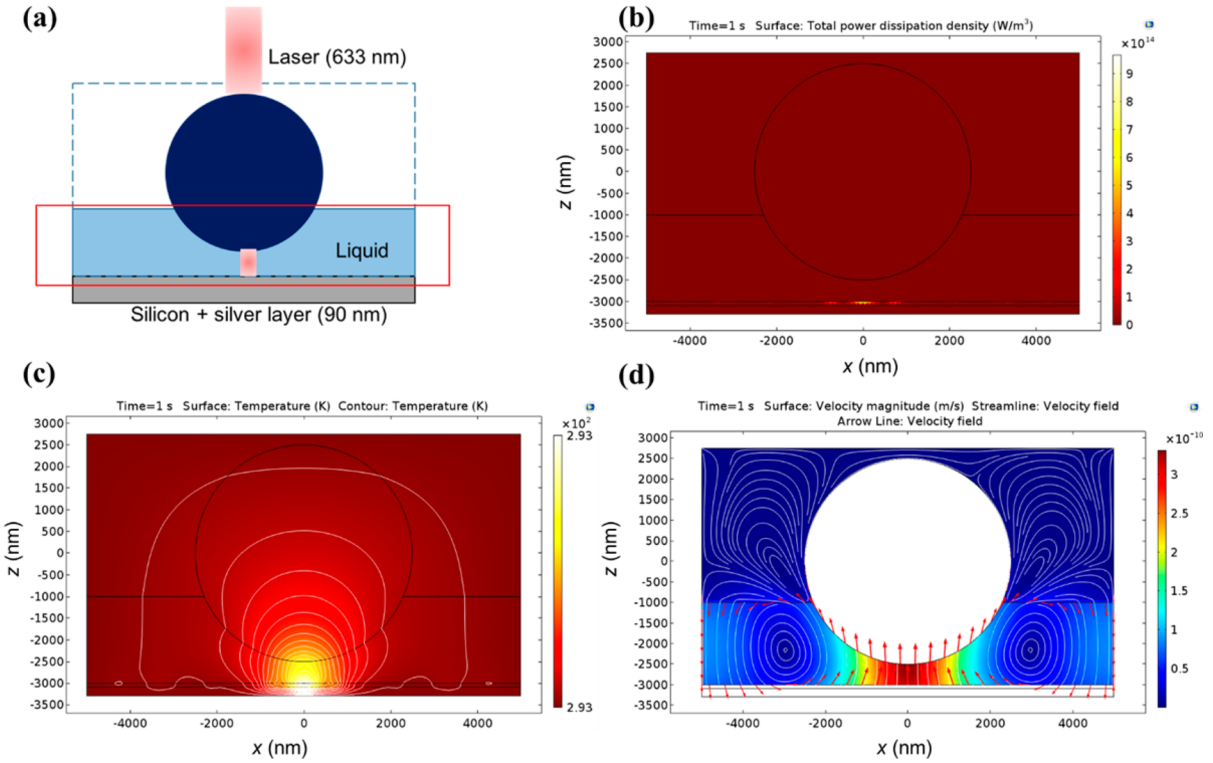

Figure 4. FEM simulation of thermal gradient effect on the SERS enhancement. (a) Schematic of the NASERS modeling setup in COMSOL Multiphysics. (b) Distribution of total power dissipation density which contributes as the electromagnetic heating source; the microsphere is shown by the black circle. (c) Temperature distribution and contours at 1 s time stamp due to the laser irradiation. (d) Magnitude of the fluid velocity (shown for the *xz*-plane) and direction of the velocity field (shown as streamline and arrow lines) considering volume force and Marangoni effect.

To investigate the effect of the increased in electromagnetic field intensity on the Raman scattering, a monolayer of 1,2-bis(4-pyridyl)ethylene (BPE) was immobilized on the SERS substrate. The monolayer of BPE was achieved by immersing the SERS substrate with 5 mM of BPE in ethanol for 24 h. To wash off the unconjugated BPE, the substrate was rinsed three times in neat ethanol solution. The substrate was dried using N_2 gas and stored in a vacuum box for further experimentation. The SERS spectra of BPE in the presence and absence of microspheres is shown in Figure 3a. The raw intensity of Raman scattering was increased 5-fold due to the presence of microspheres (nanojet effect) as shown in Figure 3a. It should also be noted that the Raman scattering response is in fact coming from smaller effective area compared to when there is no microsphere, because of the reduction in the beam width due to the presence of microsphere. Now, the enhancement factors (EF) of the nanojet SERS system can be quantified as

$$\mathrm{EF}_{\mathrm{NASERS}} = \frac{I_{\mathrm{NASERS}}/N_{\mathrm{NASERS}}}{I_{\mathrm{NRS}}/N_{\mathrm{NRS}}}$$

where I_{NASERS} and I_{NRS} are the intensities of the NASERS and normal Raman spectroscopy (NRS) signals, respectively, and N_{NASERS} and N_{NRS} are the number of molecules contributing to the NASERS and NRS signals, respectively. The enhancement factor for the nanojet SERS system with BPE as a probe molecule was found to be $\sim 1.88 \times 10^{10}$, which is about ~867 times higher than THAT without the nanojet effect on the SERS substrate[41] and $\sim 10^4$ times larger enhancement compared with commercial SERS substrates (see Supporting Information Figures S-3 and S-8 for SERS EF calculation with BPE molecule and on Klarite substrate).

In order to show that the system is capable of detecting single molecule, Rhodamine 6G (R6G) was used as a target molecule. R6G solution with varying concentrations were prepared and placed on the top of the SERS substrate. In the absence of microspheres, the SERS substrate can detect R6G molecules up to a concentration of 10^{-8} M. Figure 3b shows the comparison of SERS intensity in the absence of microspheres at different R6G concentrations. The nanojet effect and NASERS performance are shown in Figure 3c. The results show that the NASERS system can detect R6G molecules down to a concentration of 10^{-12} M. This represents four-orders of magnitude improvement in the limit of detection (see Supporting Information text and Figure S-4) due to the nanojet effect on the NASERS system. With a droplet diameter of 5 mm^2, spot size diameter of 1.25 μm^2 (Figure S-5) the average number of molecules detected can be calculated to be ~0.7 (see SERS enhancement factor calculation with R6G as a probe molecule in the Supporting Information and Figure S-7).

The improvement in the limit of detection can be understood as follows. As per the previous discussion, the R6G molecules will experience a radiation pull (~fN) toward the hot spot due to gradient forces (acting from low EM field to high EM field), a push away from the hot spot due to scattering forces, Soret force (due to temperature gradients of ~1 K/μm) which pushes the molecules away from the hot spot, and thermoplasmonic convection (~10 nm/s) which depletes molecules from the hot spot. Therefore, we expect the SERS intensity to decrease at the nanojet regions (hot spot) due to depletion of target molecules. In contrast, we observed greatly enhanced Raman signal with the NASERS setup. This enhancement phenomenon can be explained in terms of Marangoni convection. Figure 4a shows the schematic of the

DOI: 10.1021/acssensors.7b00427
ACS Sens. XXXX, XXX, XXX−XXX

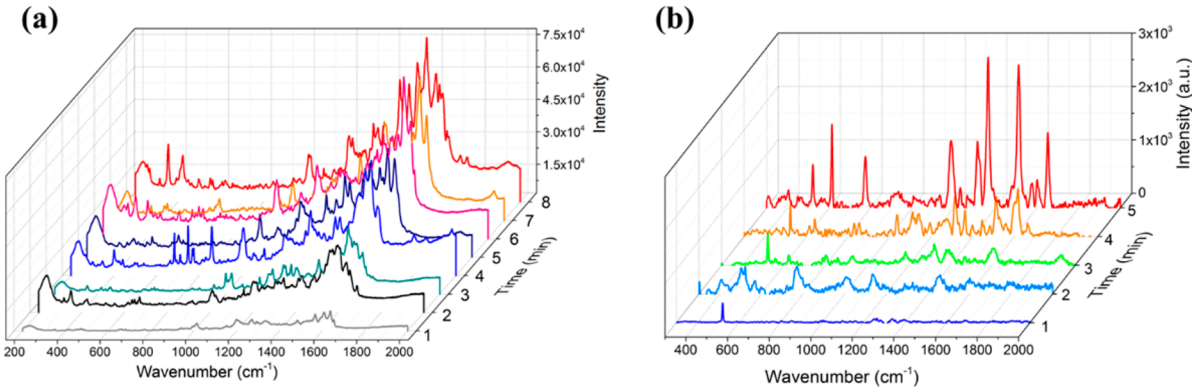

Figure 5. Time dependent NASERS for (a) BPE solution and (b) 1 μM R6G.

simulation set up. Figure 4b shows that the peak power dissipation at the plasmonic metal surface (Ag) due to photonic nanojet can be as high as ~10^{15} W/m^3. The center point under the microsphere will be the heat source due to the electromagnetic heating effect. Figure 4c shows the temperature distribution under such heat source. The temperature gradient shown in Figure 4c will contribute to two forms of motion for analytes: thermal diffusion and convection. The thermal diffusion (Soret effect) is relatively weak due to both the minimal gravitational force at such a small distance (~10 nm/s) (Figure S-6) and hence the analyte cannot move far. Figure 4d shows the highest velocity magnitude under the nanojet region when considering the Marangoni effect (~60 nm/s). Thus, Marangoni convection will be contributing more to bringing additional analytes back to the nanojet region to enrich the molecules compared to natural convection. Natural convective circulating process was oberved by Lee's group,[38] which may also contribute to the observed enhanced Raman signal. The final confirmation of recirculation current was achieved by taking time dependent Raman spectra (Figure 5) for two different molecules (BPE, R6G). Due to accumulation of new molecules over time due to Marangoni convection current, the intensity of Raman scattering increases with time (Figures 5).

In conclusion, the nanojet effect provides optical confinement of the incident field leading to ~90 times increase of the electromagnetic field intensity in addition to the normal SERS enhancement of the substrate. The enhanced electromagnetic field and confinement and enrichment of molecules result in SERS enhancement factor of ~3.58×10^{10}. The NASERS system was utilized to detect R6G molecules at picomolar concentration. The mechanism of analyte enrichment at the hot spot is explained in terms of Marangoni convection. The nanojet SERS setup provides a unique platform to perform high-resolution chemical mapping of single molecule without using scanning probe microscopy techniques which will potentially increase the throughput of single molecule chemical mapping.

■ ASSOCIATED CONTENT

Supporting Information

The Supporting Information is available free of charge on the ACS Publications website at DOI: 10.1021/acssensors.7b00427.

Description of experimental methods, equations used in the multiphysics calculations, analytical results comparing convection and diffusion velocity terms, electric field distribution for the photonic nanojet system, SERS enhancement factor (EF) calculation, calculation of limit of detection (LoD), flow distribution without Marangoni effect, comparison of single molecule and average SERS spectra, and assessing the uniformity of the SERS substrate (PDF)

■ AUTHOR INFORMATION

Corresponding Authors

*E-mail: mgartia@lsu.edu.
*E-mail: loganliu@illinois.edu.

ORCID

Xinhao Wang: 0000-0002-4050-8736
Manas Ranjan Gartia: 0000-0001-6243-6780

Notes

The authors declare no competing financial interest.

■ ACKNOWLEDGMENTS

The research reported here was supported, in part, by the Louisiana Board of Regents through the Board of Regents Support Fund (Contract Number: LEQSF(2017-20)-RD-A-04 and LEQSF(2017-18)-ENH-TR-08) and National Science Foundation (Award Number: 1660233). M.R.G. thanks Louisiana State University start-up funds for partially supporting the research.

■ REFERENCES

(1) Ambrose, W. P.; Goodwin, P. M.; Jett, J. H.; Van Orden, A.; Werner, J. H.; Keller, R. A. Single molecule fluorescence spectroscopy at ambient temperature. *Chem. Rev.* **1999**, *99* (10), 2929−2956.
(2) Anger, P.; Bharadwaj, P.; Novotny, L. Enhancement and quenching of single-molecule fluorescence. *Phys. Rev. Lett.* **2006**, *96* (11), 113002.
(3) Kinkhabwala, A.; Yu, Z.; Fan, S.; Avlasevich, Y.; Müllen, K.; Moerner, W. Large single-molecule fluorescence enhancements produced by a bowtie nanoantenna. *Nat. Photonics* **2009**, *3* (11), 654−657.
(4) Kühn, S.; Håkanson, U.; Rogobete, L.; Sandoghdar, V. Enhancement of single-molecule fluorescence using a gold nanoparticle as an optical nanoantenna. *Phys. Rev. Lett.* **2006**, *97* (1), 017402.
(5) Moerner, W.; Fromm, D. P. Methods of single-molecule fluorescence spectroscopy and microscopy. *Rev. Sci. Instrum.* **2003**, *74* (8), 3597−3619.
(6) Betzig, E.; Chichester, R. J. Single molecules observed by near-field scanning optical microscopy. *Science* **1993**, *262*, 1422−1422.
(7) Gimzewski, J. K.; Joachim, C. Nanoscale science of single molecules using local probes. *Science* **1999**, *283* (5408), 1683−1688.

DOI: 10.1021/acssensors.7b00427
ACS Sens. XXXX, XXX, XXX−XXX

(8) Xie, X. S.; Dunn, R. C. Probing single molecule dynamics. *Science* **1994**, *265*, 361−361.
(9) Celedon, A.; Nodelman, I. M.; Wildt, B.; Dewan, R.; Searson, P.; Wirtz, D.; Bowman, G. D.; Sun, S. X. Magnetic tweezers measurement of single molecule torque. *Nano Lett.* **2009**, *9* (4), 1720−1725.
(10) Hayazawa, N.; Tarun, A.; Inouye, Y.; Kawata, S. Near-field enhanced Raman spectroscopy using side illumination optics. *J. Appl. Phys.* **2002**, *92* (12), 6983−6986.
(11) Neuman, K. C.; Nagy, A. Single-molecule force spectroscopy: optical tweezers, magnetic tweezers and atomic force microscopy. *Nat. Methods* **2008**, *5* (6), 491.
(12) Nie, S.; Emory, S. R. Probing single molecules and single nanoparticles by surface-enhanced Raman scattering. *Science* **1997**, *275* (5303), 1102−1106.
(13) Kneipp, K.; Wang, Y.; Kneipp, H.; Perelman, L. T.; Itzkan, I.; Dasari, R. R.; Feld, M. S. Single molecule detection using surface-enhanced Raman scattering (SERS). *Phys. Rev. Lett.* **1997**, *78* (9), 1667.
(14) Zrimsek, A. B.; Chiang, N.; Mattei, M.; Zaleski, S.; McAnally, M. O.; Chapman, C. T.; Henry, A.-I.; Schatz, G. C.; Van Duyne, R. P. Single-Molecule Chemistry with Surface-and Tip-Enhanced Raman Spectroscopy. *Chem. Rev.* **2017**, *117* (11), 7583−7613.
(15) Jiang, S.; Zhang, Y.; Zhang, R.; Hu, C.; Liao, M.; Luo, Y.; Yang, J.; Dong, Z.; Hou, J. Distinguishing adjacent molecules on a surface using plasmon-enhanced Raman scattering. *Nat. Nanotechnol.* **2015**, *10* (10), 865−869.
(16) Zhang, R.; Zhang, Y.; Dong, Z.; Jiang, S.; Zhang, C.; Chen, L.; Zhang, L.; Liao, Y.; Aizpurua, J.; Luo, Y. e.; et al. Chemical mapping of a single molecule by plasmon-enhanced Raman scattering. *Nature* **2013**, *498* (7452), 82−86.
(17) Kneipp, K.; Kneipp, H. Single molecule Raman scattering. *Appl. Spectrosc.* **2006**, *60* (12), 322A−334A.
(18) Fan, M.; Andrade, G. F.; Brolo, A. G. A review on the fabrication of substrates for surface enhanced Raman spectroscopy and their applications in analytical chemistry. *Anal. Chim. Acta* **2011**, *693* (1), 7−25.
(19) Campion, A.; Kambhampati, P. Surface-enhanced Raman scattering. *Chem. Soc. Rev.* **1998**, *27* (4), 241−250.
(20) Willets, K. A.; Van Duyne, R. P. Localized surface plasmon resonance spectroscopy and sensing. *Annu. Rev. Phys. Chem.* **2007**, *58*, 267−297.
(21) Qian, X.-M.; Nie, S. Single-molecule and single-nanoparticle SERS: from fundamental mechanisms to biomedical applications. *Chem. Soc. Rev.* **2008**, *37* (5), 912−920.
(22) Duan, H.; Hu, H.; Kumar, K.; Shen, Z.; Yang, J. K. Direct and reliable patterning of plasmonic nanostructures with sub-10-nm gaps. *ACS Nano* **2011**, *5* (9), 7593−7600.
(23) Im, H.; Bantz, K. C.; Lindquist, N. C.; Haynes, C. L.; Oh, S.-H. Vertically oriented sub-10-nm plasmonic nanogap arrays. *Nano Lett.* **2010**, *10* (6), 2231−2236.
(24) Haynes, C. L.; Van Duyne, R. P. Plasmon-sampled surface-enhanced Raman excitation spectroscopy. *J. Phys. Chem. B* **2003**, *107* (30), 7426−7433.
(25) Chen, Z.; Taflove, A.; Backman, V. Photonic nanojet enhancement of backscattering of light by nanoparticles: a potential novel visible-light ultramicroscopy technique. *Opt. Express* **2004**, *12* (7), 1214−1220.
(26) Devilez, A.; Bonod, N.; Wenger, J.; Gérard, D.; Stout, B.; Rigneault, H.; Popov, E. Three-dimensional subwavelength confinement of light with dielectric microspheres. *Opt. Express* **2009**, *17* (4), 2089−2094.
(27) Dantham, V.; Bisht, P.; Namboodiri, C. Enhancement of Raman scattering by two orders of magnitude using photonic nanojet of a microsphere. *J. Appl. Phys.* **2011**, *109* (10), 103103.
(28) Fang, Y.; Seong, N.-H.; Dlott, D. D. Measurement of the distribution of site enhancements in surface-enhanced Raman scattering. *Science* **2008**, *321* (5887), 388−392.
(29) Blackie, E. J.; Ru, E. C. L.; Etchegoin, P. G. Single-molecule surface-enhanced Raman spectroscopy of nonresonant molecules. *J. Am. Chem. Soc.* **2009**, *131* (40), 14466−14472.
(30) Etchegoin, P. G.; Lacharmoise, P. D.; Le Ru, E. Influence of photostability on single-molecule surface enhanced Raman scattering enhancement factors. *Anal. Chem.* **2009**, *81* (2), 682−688.
(31) De Angelis, F.; Gentile, F.; Mecarini, F.; Das, G.; Moretti, M.; Candeloro, P.; Coluccio, M.; Cojoc, G.; Accardo, A.; Liberale, C.; et al. Breaking the diffusion limit with super-hydrophobic delivery of molecules to plasmonic nanofocusing SERS structures. *Nat. Photonics* **2011**, *5* (11), 682−687.
(32) Cho, H.; Lee, B.; Liu, G. L.; Agarwal, A.; Lee, L. P. Label-free and highly sensitive biomolecular detection using SERS and electrokinetic preconcentration. *Lab Chip* **2009**, *9* (23), 3360−3363.
(33) Juan, M. L.; Righini, M.; Quidant, R. Plasmon nano-optical tweezers. *Nat. Photonics* **2011**, *5* (6), 349−356.
(34) Min, C.; Shen, Z.; Shen, J.; Zhang, Y.; Fang, H.; Yuan, G.; Du, L.; Zhu, S.; Lei, T.; Yuan, X. Focused plasmonic trapping of metallic particles. *Nat. Commun.* **2013**, *4*, 2891.
(35) Roxworthy, B. J.; Bhuiya, A. M.; Vanka, S. P.; Toussaint, K. C., Jr Understanding and controlling plasmon-induced convection. *Nat. Commun.* **2014**, *5*, 3173.
(36) Choi, I.; Huh, Y. S.; Erickson, D. Size-selective concentration and label-free characterization of protein aggregates using a Raman active nanofluidic device. *Lab Chip* **2011**, *11* (4), 632−638.
(37) Donner, J. S.; Baffou, G.; McCloskey, D.; Quidant, R. Plasmon-assisted optofluidics. *ACS Nano* **2011**, *5* (7), 5457−5462.
(38) Kang, T.; Hong, S.; Choi, Y.; Lee, L. P. The effect of thermal gradients in SERS spectroscopy. *Small* **2010**, *6* (23), 2649−2652.
(39) Duhr, S.; Braun, D. Why molecules move along a temperature gradient. *Proc. Natl. Acad. Sci. U. S. A.* **2006**, *103* (52), 19678−19682.
(40) Ndukaife, J. C.; Kildishev, A. V.; Nnanna, A. G. A.; Shalaev, V. M.; Wereley, S. T.; Boltasseva, A. Long-range and rapid transport of individual nano-objects by a hybrid electrothermoplasmonic nanotweezer. *Nat. Nanotechnol.* **2015**, *11*, 53−59.
(41) Chang, T.-W.; Gartia, M. R.; Seo, S.; Hsiao, A.; Liu, G. L. A wafer-scale backplane-assisted resonating nanoantenna array SERS device created by tunable thermal dewetting nanofabrication. *Nanotechnology* **2014**, *25* (14), 145304.

DOI: 10.1021/acssensors.7b00427
ACS Sens. XXXX, XXX, XXX−XXX